

Assessing grain size distribution characteristics of debris flow torrents using UAV photogrammetry

Debris flow, Grain size, UAV photogrammetry, BASEGRAIN

*Samikshya Dahal¹, Fumitoshi Imaizumi², Shoki Takayama²

1. Graduate School of Integrated Science and Technology, Shizuoka University

2. Faculty of Agriculture, Shizuoka University

1. Introduction

Debris flow is significant geohazard in mountainous regions that pose a serious threat to people's life and property. Debris flow ranges from mudflows and lahars with a high fraction of fine particles such as clay, silt, and sand, to granular flows containing significant coarse particles, some exceeding a meter in diameter (Phillips and Davies 1991). Investigating the spatio-temporal changes in grain size within debris flow channels is necessary for understanding the dynamics of debris flows and their potential downstream impacts. This study aims to measure distributions of boulders in the debris flow torrent of the Ohya landslide in central Japan using UAV-based Structure from Motion (UAV-SfM) photogrammetry for capturing aerial images and granulometric analysis using BASEGRAIN software.

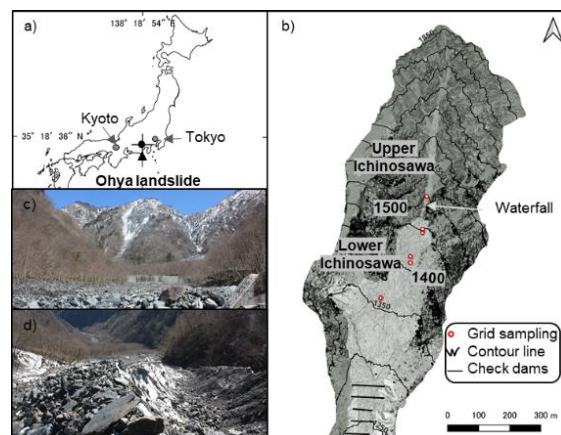


Fig. 1 Map and photographs of Ichinosawa catchment in Ohya landslide, central Japan

2. Methodology

The study was conducted in Ichinosawa catchment in the northern part of Ohya landslide, central Japan (Fig. 1). The Ichinosawa catchment comprises upper Ichinosawa, debris-flow initiation zone, and lower Ichinosawa, transportation and deposition zones (Imaizumi et al. 2005). UAV photographs captured before and after debris flow events on April 21, 2021, and August 24, 2021, and before and after sediment supply seasons on August 24, 2021, and April 22, 2022, were used to analyze the effect of debris flow and sediment supply on the grain size of deposits. Photographs taken using DJI Phantom 4 RTK drone were processed using Agisoft Metashape Software to create orthomosaics and DEM. In upper Ichinosawa, orthomosaics were extracted at 10-m intervals along the channel based on slope gradient, while in lower Ichinosawa, multiple 10x10 m areas were extracted in the channel based on DEM of difference (DoD). These clipped images were then analyzed using BASEGRAIN software to calculate the coverage ratio of boulders. The ratio of surface coverage ($R_{BG,x}$) for sediments larger than size threshold x mm in BASEGRAIN was calculated by dividing the total area of sediment greater than x mm (A_x) by the total area of the analysis site (A_{total}). Validation was conducted using grid sampling with 6 sections of 10 x 10 m (100 m² in area). The coverage ratio was calculated by dividing the total number of sediments larger than x (N_x), by the total number of sediments sampled (N_{total}). Impact of image resolution was also assessed using photographs captured from 80 m and 15 m altitude.

3. Result

3.1. Detection of boulders using BASEGRAIN

Surface coverage ratio of larger sediment particles obtained by BASEGRAIN analysis was different between the high and low altitude photographs (80 and 15 m above the ground, respectively; Fig. 2). BASEGRAIN shows better performance in detecting finer-sized sediments in photographs captured from lower altitude (Fig. 2). However, this advantage is accompanied by a potential drawback; the algorithm overlooks larger sediments (Fig. 3). On the other hand, when employing photographs taken from the higher altitude, BASEGRAIN tends to miss

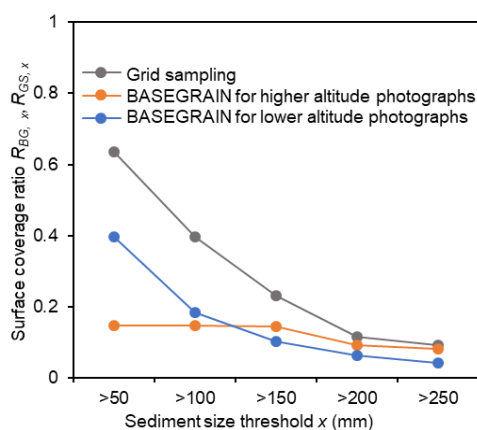


Fig. 2 Surface coverage of sediments for different altitude greater than the threshold size

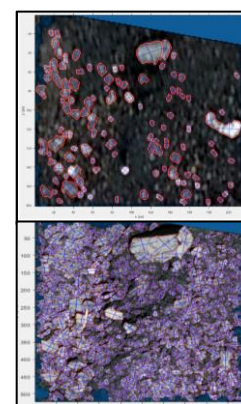


Fig. 3 Detection of sediment from higher altitude (up) and lower altitude photographs (down).

finer sediments but exhibits greater accuracy in detecting coarser sizes (>250 mm) (Fig. 2). When comparing the results for surface coverage by different sediment size threshold, BASEGRAIN and grid sampling data for sediments greater than 250 mm showed great alignment (Fig. 4).

3.2. Spatio-temporal changes in the boulder size

The spatial distribution of boulders along the debris flow channel section shows considerable variation across different analysis periods (Figs. 5, 6). Boulder ratio is comparatively higher just below the waterfall zone at the centre of study site than downstream area. This is because, below the waterfall, in lower Ichinosawa, channel gradient starts to decrease, slowing down the flow velocity. This likely causes selective sorting, with large boulders settling while finer particles are transported downstream with muddy flows. During the debris flow season, there was an increase in boulder ratio in upper Ichinosawa, while it decreased in almost all parts of lower Ichinosawa, remaining relatively constant in the end zone of the debris flow channel (Fig. 5). This is due to selective transport of fine sediments from upper to lower region (Imaizumi et al. 2005). In the upper section of upper Ichinosawa, due to significant sediment erosion, boulder ratio increased, and channel got narrowed due to deepening of channel (Fig. 5). The sediment supply season led to an overall increase in boulder coverage on the surface of the debris flow channel with significant increase in middle section of upper Ichinosawa due to active boulder supply from surrounding active hillslopes.

4. Conclusion

Combined use of BASEGRAIN software and UAV photogrammetry can be valuable solution for analyzing boulder-sized sediments in physically inaccessible areas. In Ohya Landslide, there is significant differences in boulder distribution between the upper and lower catchments across different seasons due to difference in channel morphology and heterogeneous sediment supplies from adjacent hillslopes. The spatial distribution of boulders in debris flow channels reveals insights into the behavior of past debris flows. Therefore, investigating their spatial distribution and change patterns is crucial for planning effective mitigation and prevention measures.

References

- Imaizumi F, Tsuchiya S, Osaka O (2005) Behaviour of debris flows located in a mountainous torrent on the Ohya landslide, Japan. *Canadian Geotechnical Journal* 42:919–931.
- Phillips CJ, Davies TRH (1991) Determining rheological parameters of debris flow material. *Geomorphology* 4:101–110.

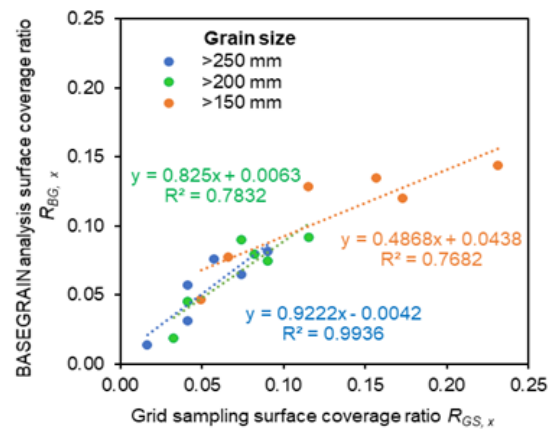


Fig 4 Surface coverage ratio between grid sampling and BASEGRAIN (high altitude)

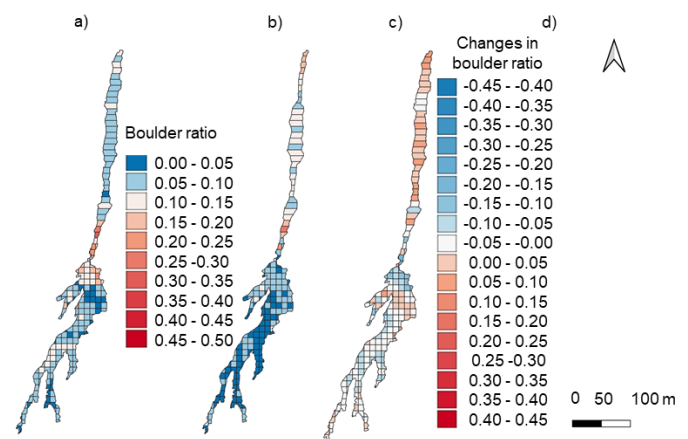


Fig. 5 Changes in the boulder ratio in debris flow season: **a** on April 21, 2021, prior to the debris flow season. **b** on August 24, 2021, after the debris flow season. **c** temporal changes in boulder ratios

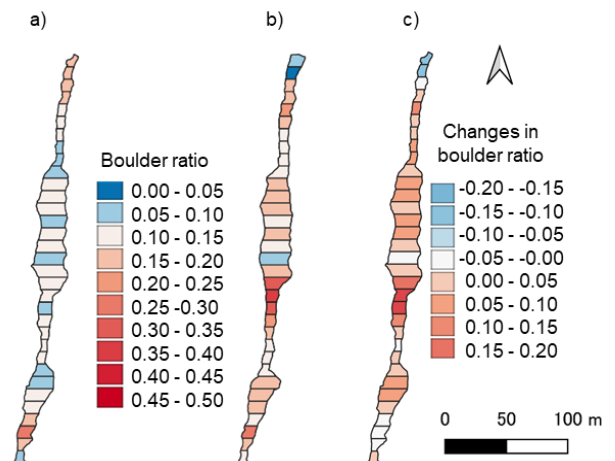


Fig. 6 Changes in the boulder ratio in sediment supply season in upper Ichinosawa: **a** on August 24, 2021, prior to the sediment supply season. **b** on April 22, 2022, after the sediment supply season. **c** temporal changes in boulder ratios